Characterization of thermal conductivity of backfill materials for UPCS by various methods: lab, in situ and numerical analysis

Ba Huu Dinh[1], *Cong-Hanh* Nguyen[2], *Young-Sang* Kim[2#], *Gyeong-O* Kang[3]

[1]*Basic Research Laboratory (BRL), Department of Civil Engineering, Chonnam National University, Yongbong-ro 77, Buk-gu, Gwangju 61186, South Korea.*
[2]*Department of Civil Engineering, Chonnam National University, Yongbong-ro 77, Buk-gu, Gwangju 61186, South Korea.*
[3]*Department of Civil Engineering, Gwangju University, 277 Hyodeong-ro, Nam-gu, Gwangju, South Korea*
[#]*Corresponding author: geoyskim@jnu.ac.kr*

ABSTRACT

This research evaluates the thermal properties of the proposed backfill materials (prepacked concrete (PAC)) that function as the heat release medium for the underground power cable system (UPCS). First, a hot disk sensor was used to measure the thermal conductivity of small-scale backfill materials in the laboratory. The horizontal thermal response test (TRT) was then performed with a 5 × 3 × 2 m full-scale sample for the in-situ evaluation. Afterward, the data from the TRT was utilized to couple with the infinite line source model (ILS) to predict the thermal conductivity of the full-scale sample. Finally, the thermal conductivity of the PAC was back-calculated using COMSOL Multiphysics. All these tests were also performed with natural sand (conventional backfill material) to compare with the PAC. Thermal conductivities calculated by numerical simulation and the ILS model were in good agreement (difference < 3%), demonstrating that the proposed ILS model coupled with horizontal TRT data is appropriate for estimating the thermal conductivity of full-scale backfill material in situ. The results of three testing methods indicated that the prepacked concrete has a high thermal conductivity (> 2 W/(mK)), thus satisfying the heat release ability requirement for the UPCS. The laboratory test slightly underestimated the thermal conductivity (less than 8%) compared to the estimated values from the ILS model and numerical model involving prepacked concretes; however, natural sand showed a significant difference (1.365 W/(mK) and 1.8 W/(mK), 32 %) attributed to the influence of the water content change during the TRT. Therefore, it is recommended that the in-situ testing conditions should be considered for the sand (or soils) to avoid the overestimation or underestimation of their thermal conductivity.

Keywords: Underground power cable system; backfill materials; thermal response test; thermal conductivity.

1. Introduction

Alongside the development of society, the demand for electrical energy is increasing. Nevertheless, the traditional power transmission system (overhead transmission cable lines) not only diminishes urban beauty but also encroaches upon living space, particularly in densely populated cities [1,2]. Over the past few decades, underground power cable systems (UPCS) have been widely researched and utilized to overcome the inherent disadvantages of traditional power transmission lines.

The unsaturated soils have low thermal conductivity, mostly lower than 1.0 W/(m.K) [3,4] (namely at depths of lower than 2 m, where UPCS is usually installed) [5]. UPCS operation can generate a very large amount of heat [6,7]. If that amount of heat is not dissipated, it may cause overheating of the cable, resulting in a fire and disruption of the power transmission line. Therefore, thermal backfill materials with high thermal conductivity are developed and utilized for heat dissipation from cable to ground [8,9].

In recent years, many types of backfilling materials have been researched and proposed to be used as the thermally enhanced material for the UPCS. Notably, fluidized formula backfills, the commonly used materials, have a high flowability and water fraction, which ensures that the mixture fills the trench without the need of compaction [9, 25–27]. Due to the use of a lot of water, fluidized formula backfills when in an unsaturated state have a much lower thermal conductivity than in a saturated state [10]. There is another problem when using this type of material: during backfilling, the liquid material causes a buoyancy force, leading the UPC to move upward and result in a change in position compared to the original design. This study proposes a material (prepacked aggregate concrete (PAC)) to address the drawbacks of conventional backfill materials and fluidized formula backfills. PAC consists of two main components: grout and coarse aggregate. Coarse aggregate is placed first to fix the position of the UPC by its own gravity to avoid the flow-up of the UPC caused by buoyancy force. Afterward, grout with high workability is injected to fill the gaps between the coarse aggregates. It should be noted that aggregates typically

have high thermal conductivity and low water absorption [11,12]; therefore, using coarse aggregate and grout together creates a mixture with a lower water content than using grout only. Thus, it is expected that PAC has higher thermal conductivity even under unsaturated conditions.

This study evaluates the feasibility of using a new type of backfill material through physical properties and thermal conductivity. First, general properties such as flowability (for grout), unconfined compressive strength, and bleeding, are tested. Then, its thermal conductivity properties are evaluated through three methods: (1) laboratory experiment using Hot Disk M1 equipment; (2) proposing to use an infinite line source model (ILS) combined with TRT in the field (full-scale test bed); (3) using a finite element coded program (numerical model) to back calculations. The consistency in thermal conductivity of material is examined using measurement results in laboratory conditions with small samples and in situ working conditions (full-scale test samples).

2. Study program

2.1. Materials

The raw materials for the PAC include coarse aggregate (i.e., gravel) and grout. The gravel diameter was 25 mm with a porosity of 49% - 55% depending on the degree of rod compaction. Meanwhile, for the grout of PAC, fly ash; commercialized ultrarapid-setting cement (URSC); and quartz sand with a particle size ranging from 0.075 mm to 0.22 mm (70-200 mesh) were used.

The percentage of water to solid materials in the high-flowable grout (for PAC) was controlled within 22–25%. The solid material was made up of quartz powder and binder in a 1:2 ratio. The binder consists of fly ash and URSC with a ratio of 1:0.1.

In this study, natural sand with a specific gravity of 2.65 and a maximum diameter of 0.22 mm was used as reference backfill material to compare with the proposed backfill material.

2.2. Experimental methods

2.2.1. Measurement of thermal properties for specimens

Fig. 1 presents the thermal conductivity measurement equipment. For the natural sand and surrounding soil, thermal conductivities were measured using a commercial thermal properties analyzer (KD2 pro). The dual needle with 30 mm long and 1,3 mm diameter was used. The test was conducted following ASTM D5334 standards [13]. Regarding the PAC sample, the thermal conductivity was measured using the Hot Disk M1 devices. This test is performed in accordance with the ISO 22007-2: 2015 standard [14]. A Kapton sensor with a diameter of 2 cm was employed. The thermal conductivity of each sample was measured three times to ensure the reliability of the results. Notably, for the hot disk type, the smooth surface of the sample must be prepared to ensure the perfectly interaction between the Kapton sensor and sample surface.

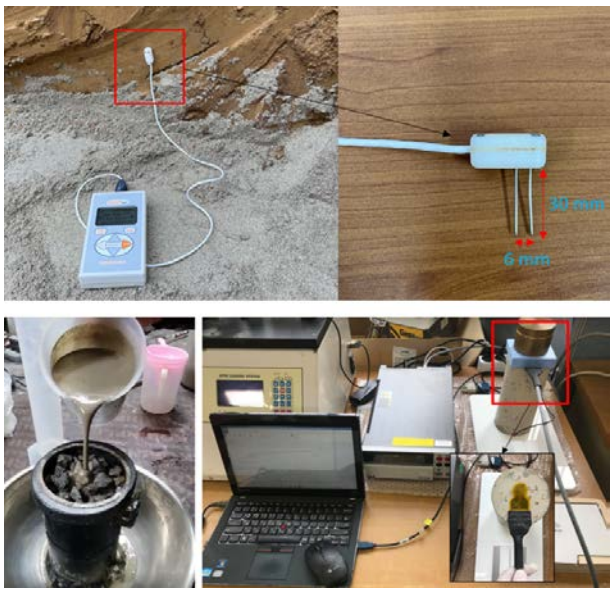

Figure 1. (above) KD2 pro, (bellow) Hot Disk M1

2.2.2. Thermal properties in-situ measurement using thermal response test (TRT)

The TRT setup was used to estimate the thermal conductivity of full-scale backfill material samples (Figure 2). The test device includes a pump, flow meter, heater, data logger, and RTD sensors. The pump used to circulate the water has a maximum capacity of 100 L/min. The flow meter was used to measure the flow rate of the water. The heater with a maximum capacity of 5 kW was used to increase the water temperature. In this study, the heat input power and the flow rate were kept constant at 1.5 kW and 8-9 l/min, respectively. The RTD sensors were used to measure the inlet and outlet water temperature and the backfill material temperature (at the different depths of 0 m, 0.6 m, 1.9 m, 2.6 m). All the data (flow rate and temperature of water and backfill materials) were recorded using the datalogger with the interval of 3 min. The test was performed continuously for more than 48 hours (2 days), and the data of the test was used to estimate the thermal conductivity of backfill materials using ILS model.

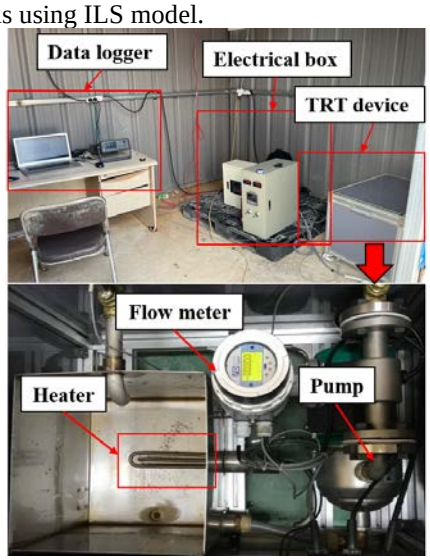

Figure 2. Thermal response test set up

Figure 3 shows the TRT construction process. The trench with the dimensions of 5 × 2 × 3 m (length × width × depth) is prepared for each backfill material (natural

sand and PAC). For both cases, the TRT steel pipe (diameter of 20 mm) was installed at a depth of 1.9 m and the UPCS was buried at a depth of 1.2 m from the ground surface. For the natural sand, the compaction is divided into 3 layers. The thermal conductivity of each layer of natural sand and surrounding soil is measured using the KD2 pro thermal analyzer (Figure 3(a–c)). This thermal conductivity then was used as the input data for the numerical model. Regarding the PAC, the trench was prepacked with the gravel, then the grout was mixed and poured directly into fill the trench (Figure 3(d–f)).

Figure 3. (a–c) TRT set up for natural sand: (a) measurement of thermal properties of soils using KD2 Pro, (b) steel pipe GHE backfilled with sand, (c) compaction of sand, (d–e) TRT set up for prepacked concrete: (d) installing UPCS, (e) The trench filled with gravel, (f) The trench filled with grout

2.2.3. Infinite line source model for calculating the thermal conductivity from TRT data

ILS model is well known as a simple and convenient model used to estimate the thermal conductivity of the soil as well as evaluate the heat transfer performance of the vertical borehole heat exchanger [15]. In this study, the ILS model is proposed to estimate the thermal conductivity of the full-scale backfill material using horizontal TRT data. The average temperature of the circulating water (inlet and outlet), T_f, is determined as follows:

$$T_f = \frac{Q}{4\pi\lambda L}\ln t + \frac{Q}{4\pi\lambda L}\left(\ln\frac{4\alpha}{r_b^2} - \gamma\right) + \frac{Q}{L}R_b + T_o \quad (1)$$

where λ is thermal conductivity (W/(m.K)), Q is averaged heat exchange (W), L is the length of TRT trench (i.e., 4.75 m for this study), α is the thermal diffusivity (m^2/s), R_b is the borehole thermal resistance (mK/W), T_0 is the initial ground temperature (^oC). If $A = (Q/L)/(4\pi\lambda)$ and $B = A\ln(4\alpha/r_b^2 - \gamma) + (Q/L)R_b + T_o$, Eq. (1) is expressed as:

$$T_f = A\ln t + B \quad (2)$$

Once A is determined, the thermal conductivity of the ground can be determined as follows:

$$\lambda = \frac{Q}{L4\pi A} \quad (3)$$

It should be noted that the important assumption when using the ILS model is the initial ground temperature of the ground is constant during the TRT. To confirm that assumption, the RTD sensors were installed at different depths (0.6 m, 1.9 m, and 2.6 m) to examine the change in backfill material temperature during the TRT, as mentioned above.

2.3. Numerical method

To confirm the thermal conductivity measurement results of TRT and laboratory tests, the numerical analysis was employed as a back-calculation method. The inlet water temperature from the TRT and different thermal conductivity values were used as the input data. As a result of the numerical model, the outlet water temperature corresponding to each thermal conductivity value was obtained and compared with the outlet fluid temperature from the TRT results. Afterward, the relative error of the outlet water temperature between TRT and numerical analysis for each thermal conductivity value is calculated. The optimum thermal conductivity value then was determined corresponding to the thermal conductivity that has the lowest error of the outlet fluid temperature between TRT and numerical analysis results.

Table 1. Thermal properties of materials used for numerical model

Material	ρ (g/cm^3)	C_p (J/kgK)	λ (W/mK)	D (mm^2/s)
Soil layer 1	1888	1685	1.604	0.567
Soil layer 2	1999	1823	1.351	0.371
Soil layer 3	1708	1768	1.517	0.497
*Steel pipe	7.93	460-502	16.2	-
*Polyethylene pipe	0.950	1.55	0.34	-
Natural sand	1900	850	1.5 – 1.9	0.658
PAC	2150	950	1.8 – 2.4	0.968

*Note: provided by the manufacturer

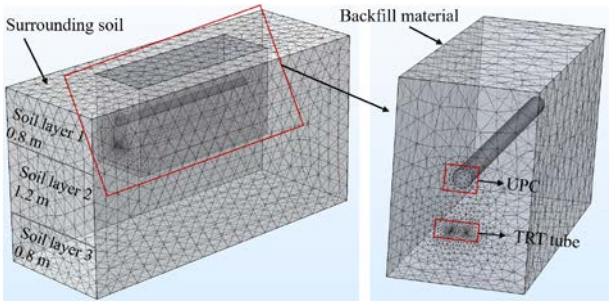

Figure 4. Numerical model

The boundary conditions for the numerical model are Dirichlet for the top and adiabatic for the lateral and bottom. The thermal properties and the initial temperature of the surrounding soil were obtained from the KD2 pro and RTD sensors, which were measured right before and during the TRT (as presented in Figure 3). Table 1 lists the thermal properties of the materials used as the input data for the numerical model.

The heat exchange process of TRT contains heat conduction between the backfill material, surrounding soil, and pipe wall, and the convection heat of the water circulating in the TRT pipe. In this study, a finite element code program (COMSOL Multiphysics) [16] coupled

with computational fluid dynamics analysis was used to simulate the heat transfer process during TRT (Figure 4). The heat conduction between the solid medium is expressed as [17]:

$$\rho C_P \frac{\partial T}{\partial t} + \nabla\left(-\lambda \nabla T\right) + Q_{\text{int}} = 0 \quad (4)$$

where ρ is density (kg/m^3), C_p is specific heat capacity (J/(kg.K)), λ is thermal conductivity (W/(m.K)), T is temperature (K), t is time (s), and Q_{int} is the heat source (W/m^3).

The energy equation of the circulating water in a TRT pipe can be expressed as [16,17]:

$$\rho_f A_p C_p \frac{\partial T_f}{\partial t} + \rho_f A_p C_p u \cdot \nabla T_f = \nabla \cdot (\lambda_f A_p \nabla T_f) + \frac{1}{2} f_D \frac{\rho A_p}{2 d_h} |u| u^2 + q + q_{wall} \quad (5)$$

where f_D is the coefficient of friction, u is velocity field, A_p is pipe cross-section area (m^2), d_h is the mean hydraulic diameter (m). In addition, q is the regular heat injection (W/m), and q_{wall} is the heat exchange through the pipe wall (W/m), which is calculated as follows [16,17]:

$$q_{wall} = (hZ)_{eff} \left(T_p - T_f\right) \quad (6)$$

where h is the heat transfer coefficient of pipe (W/(m^{2}K)), Z is the wetted perimeter of pipe (m), T_p is the temperature of the pipe wall (K), and T_f is the fluid temperature (K).

3. Result and discussion

3.1. General properties of PAC

Table 2 lists the general properties of the newly proposed backfill material. The average bleeding rate of PAC is 1.7 %, thus, classified as the normal bleeding level and satisfies the requirement according to ACI 229R-99 [18,19]. Furthermore, the grout used for PAC is 382 mm, classifying as a high flowability and pumpability backfill material [18,19]. The average compressive strength of the PAC after 28 days is 1.56 MPa, thus, satisfying the strength requirement for general backfill application purposes. It should be noted that the proposed material has an excavation ability; therefore, it is helpful in case the future repair or the new installation of the UPCS is required.

Table 2. General properties of newly proposed backfill material

Sample No.	Bleeding rate (%) (1)	Flowability (mm) (2)	Compressive strength, 28 d (MPa) (1)
1	1.5	385	1.54
2	1.8	380	1.56
3	1.8	382	1.58
Average	1.7	382	1.56
Standard	ASTM C 940 [20]	ASTM D 6103 [21]	ASTM C 39 [22]

*Note: (1) For the mixture, (2) For the grout only.

3.2. Thermal conductivity comparison

3.2.1. Thermal conductivity from TRT

Figure 5 presents the ambient temperature and the backfill material during the TRT at the depths of 0.6m, 1.9 m, and 2.6 m from the ground surface. The results show that although the ambient temperature has a large difference between day and night, the backfill material is constant even at shallow depths as 0.6 m. These results demonstrated that the effect of the surface temperature can be neglected during the short time test of TRT (i.e., 50 h).

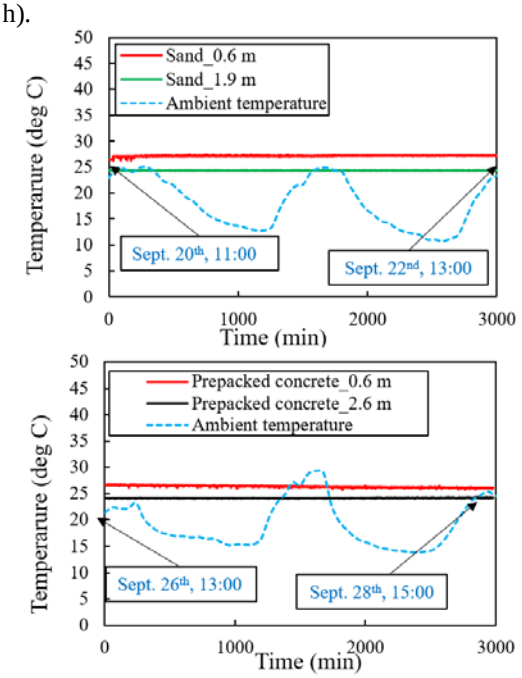

Figure 5. The ambient temperature and the backfill material temperature during the TRT

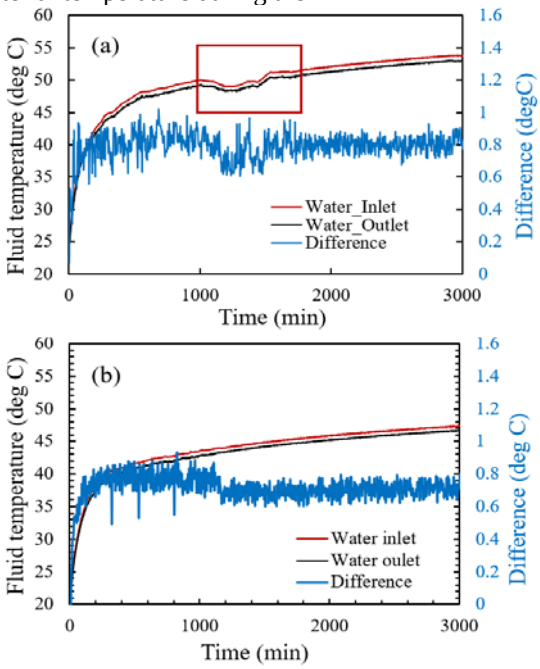

Figure 6. Outlet and inlet water temperature of TRT for (a) natural sand, and (b) PAC.

Figure 6 presents the inlet and outlet water temperature of the natural sand and PAC from the TRT. The water temperature of the natural sand case increased

then significantly decreased at the time of 1100 min. This result is caused by the different temperatures of the day and night. As a solution, the TRT box (Figure 2) is thermally insulated by using the thermal insulated material with a thickness of 10 mm and a thermal resistance of 27.8 mK/W. Consequently, the decrease in water temperature did not occur for TRT test of the PAC.

To calculate the Q in the Eq. (3), the inlet and outlet fluid temperature, (Figure 6) and the flow rate from TRT were employed.

$$Q = mC_p(T_{in} - T_{out}) \quad (7)$$

where Q is the heat input (W); m is the flow rate (kg/s); C_p is the specific heat capacity of the fluid (J/(kg.K)); and T_{in} and T_{out} are the inlet and outlet fluid temperatures, respectively.

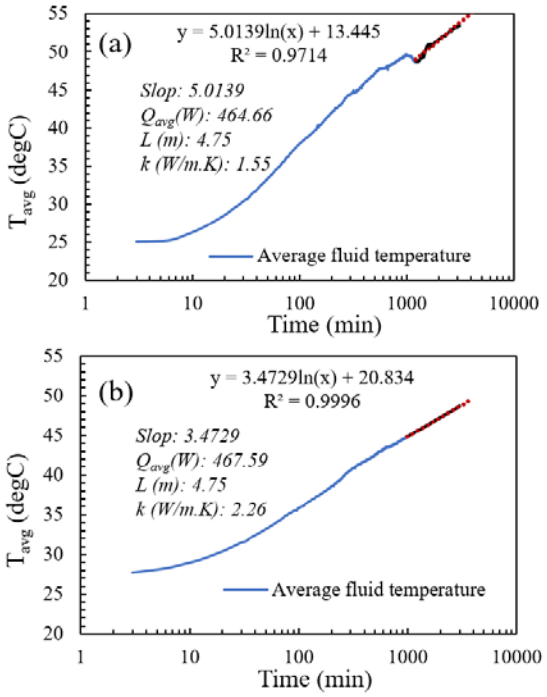

Figure 7. Average water temperature versus *ln* time of (a) natural sand and (b) prepacked concrete.

Figure 7 shows the average water temperature change with the time on the natural log scale. Please note that for the ILS model theory, the initial data should be detected for the calculation to reduce the error [23]. In other words, only the linear relationship data between T_{avg} and the time in the log scale should be used to determine slope A in Eq. (3). In this study, the linear relationship was achieved after 20 h for both natural sand and PAC. The slope A is 5.0139 (R^2 = 0.9714) and 3.4729 (R^2 = 0.9996) for the natural sand and PAC, respectively.

The thermal conductivity change with time is presented in Figure 8. For the PAC, the thermal conductivity decreases slightly and reaches the constant value after 12 h. However, the thermal conductivity of the natural sand significantly decreases from 2.1 W/(mK) (10 h) to 1.5 W/(mK) (19 h) then increases again and reaches the constant value after 25 h (1.8 W/(mK)). The reason for the variation over time of thermal conductivity of natural sand is attributed for the change in temperature in TRT box caused by the different temperatures of the day and night, as mentioned above (Figure 6(a)). The results also indicated that the thermal conductivity of the proposed backfill material was significantly higher than that of the soil (1.3 W/mK) and conventional backfill material (e.g., natural sand (1.8 W/mK)).

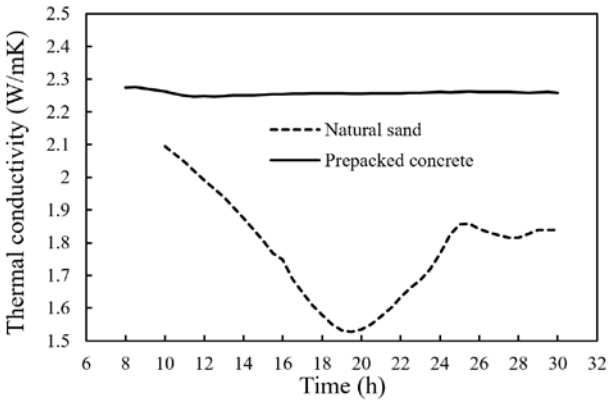

Figure 8. Thermal conductivity calculated for different testing times.

3.2.2. Thermal conductivity estimation using numerical analysis

The outlet fluid temperature of the numerical model (at different thermal conductivities of the backfill material) and TRT results are presented in Figure 9 (for natural sand) and Figure 10 (PAC). Owing to the cooling model, it is obvious that the higher the thermal conductivity, the lower the outlet fluid temperature is achieved. Figure 11 shows the relative error in the fluid temperature of experimental results (TRT) and numerical model. The results show that natural sand with a thermal conductivity of 1.8 W/(mK) and the PAC with a thermal conductivity of 2.2 W/(mK) have the lowest relative error. These results strongly agree with the estimation results using the TRT coupled ILS model.

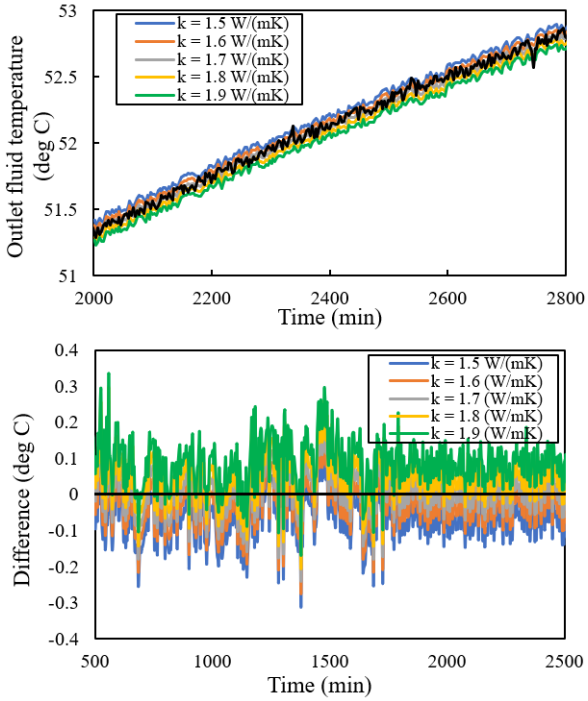

Figure 9. Outlet water temperature at the different thermal conductivity of the natural sand.

Table 3. Thermal conductivity measurement results from difference methods

Backfill material	Laboratory test (KD2 Pro & Hot disk M1)	TRT (ILS model)	Numerical analysis (Back calculation)
Natural Sand	1.365*	1.84	1.8
PAC	2.094	2.26	2.2

*Measured by KD2 Pro

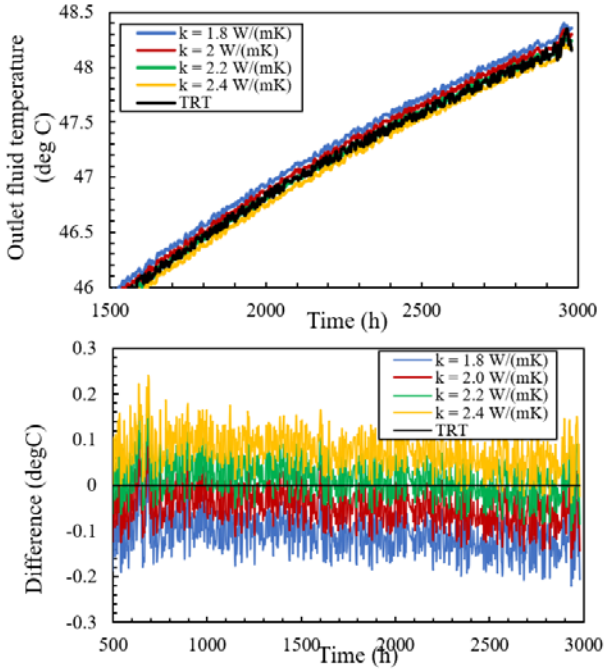

Figure 10. Outlet water temperature at the different thermal conductivity of the PAC.

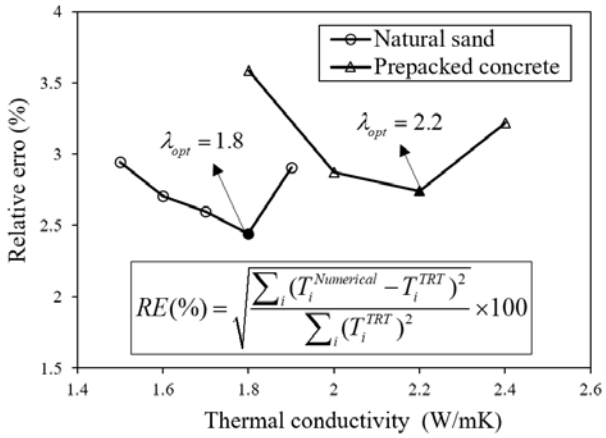

Figure 11. Relative error of outlet fluid temperature between the numerical analysis and experiment results the mixture.

The obtained results of thermal conductivity from different methods (laboratory test, TRT coupled ILS model, and numerical model) are summarized in Table 3. Regarding the PAC, thermal conductivity measurement results have good agreement between all testing methods. The maximum difference is 7.9 % (i.e., 2.094 W/(mK) for laboratory test and 2.26 W/(mK) for TRT). For the natural sand case, the thermal conductivity measured by TRT couple ILS model and numerical model has a low difference of 2.2 % (1.84 W/(mK) for TRT and 1.8 W/(mK) for numerical model); however, a significant difference (around 32%) was observed between these methods and the laboratory test (1.365 W/(mK)). This difference is attributed to the change in the degree of saturation of the natural sand during the TRT operation caused by the rainfall infiltration. It should be noted that the thermal conductivity of soil, especially the high permeability soil (i.e., sandy soil) is strongly affected by its degree of saturation. Due to the fact that the thermal conductivity of the water is about 24 times higher than that of the air; therefore, an increase in the degree of saturation (water content) of backfill material leads to a significant increase in its thermal conductivity [10, 19]. This result implied that the testing conditions in situ and laboratory should be considered to avoid the wrong estimation of the thermal conductivity and heat dissipation performance of the backfill material, especially in the case of sandy soil.

4. Conclusions

This study evaluates the thermal and mechanical properties of the thermal backfill material used to dissipate the heat generation from the UPCS. Three thermal conductivity measurement methods were employed to examine the consistency of the thermal conductivity measurement results. The results indicate that the proposed backfill material (PAC) satisfied the requirement for general backfill purposes. The grout used with high flowability of 382 mm; thus, easy to fill the space between the coarse aggregate. In addition, the strength of the PAC is 1.56 MPa, thus, can be considered as an excavatable material and helpful in case of future excavation and new installation of the cable is required.

Regarding the PAC, TRT coupled ILS model shows a very good agreement in thermal measurement results with the laboratory test and the numerical model. However, for the natural sand, the big difference in the thermal conductivity test results between the laboratory test and other methods (32 %) was caused by the rainfall infiltration. These results implied that the weather conditions should be considered during the thermal conductivity estimation process to avoid the wrong evaluation of the heat dissipation ability of the backfill materials.

Furthermore, the thermal conductivity of PAC is 2.2 W/(m.K), which is significantly higher than that of the soil (1.3 W/(m.K)) and conventional backfill material (e.g., fluidized formula backfills of 1.4 W/(m.K) [28] and natural sand of 1.8 W/(m.K)). Therefore, it is concluded that PAC is feasible to use as a heat-dissipating medium for the UPCS.

Acknowledgements

This work was supported by the Basic Research Laboratory (BRL) research grant from the National Research Foundation of Korea (NRF) (No. 2022R1A4A1033838) and the Korea Agency for Infrastructure Technology Advancement (KAIA) (No. 22RITD-C162545-0240982119420002).

References

[1] Ocłoń, P., M. Bittelli, P. Cisek, E. Kroener, M. Pilarczyk, D. Taler, R.V. Rao, A. Vallati. 2016. The performance analysis of a new thermal backfill material for underground power cable system, Appl Therm Eng. 108 (2016) 233–250. https://doi.org/10.1016/j.applthermaleng.2016.07.102.

[2] Dai, D., X. Zhang, J. Wang. 2014. Calculation of AC resistance for stranded single-core power cable conductors, IEEE Trans Magn. 50 (2014). https://doi.org/10.1109/TMAG.2014.2326040.

[3] He, H., L. Liu, M. Dyck, B. Si, J. Lv. 2021. Modelling dry soil thermal conductivity, Soil Tillage Res. 213 (2021) 105093. https://doi.org/10.1016/j.still.2021.105093.

[4] Dinh, H.B., G.H. Go, Y.S. Kim, Performance of a horizontal heat exchanger for ground heat pump system: Effects of groundwater level drop with soil–water thermal characteristics, Appl Therm Eng. 195 (2021) 117203. https://doi.org/10.1016/j.applthermaleng.2021.117203.

[5] Dinh, H.B., Cong-Hanh Nguyen, Hyeong-Ki Kim, Young-Sang Kim, Consistency in thermal conductivity measured via lab-, field-scale test, and numerical simulation for newly developed backfill materials for underground power cable system, Thermal Science and Engineering Progress, 46 (2023) 102205.

[6] Jamali-Abnavi, A., H. Hashemi-Dezaki, A. Ahmadi, E. Mahdavimanesh, M.J. Tavakoli, Harmonic-based thermal analysis of electric arc furnace's power cables considering even current harmonics, forced convection, operational scheduling, and environmental conditions, International Journal of Thermal Sciences. 170 (2021) 107135. https://doi.org/10.1016/j.ijthermalsci.2021.107135.

[7] Qin, S., Q. Xu, Q. Wang, J. Zhang, Z. Ju, Z. Hou, H. Lian, T. Wu, J. Zhang, Study on temperature rise characteristics of 110 kV XLPE cable under different service years considering dielectric loss, Energy Reports. 8 (2022) 493–501. https://doi.org/10.1016/j.egyr.2022.09.153.

[8] Ocłoń, P., P. Cisek, D. Taler, M. Pilarczyk, T. Szwarc, Optimizing of the underground power cable bedding using momentum-type particle swarm optimization method, Energy. 92 (2015) 230–239. https://doi.org/10.1016/j.energy.2015.04.100.

[9] Ocłoń, P., P. Cisek, M. Pilarczyk, D. Taler, Numerical simulation of heat dissipation processes in underground power cable system situated in thermal backfill and buried in a multilayered soil, Energy Convers Manag. 95 (2015) 352–370. https://doi.org/10.1016/j.enconman.2015.01.092.

[10] Dinh, B.H., Y.S. Kim, G. o. Kang. 2020. Thermal conductivity of steelmaking slag-based controlled low-strength materials over entire range of degree of saturation: A study for ground source heat pump systems, Geothermics. 88 (2020) 101910. https://doi.org/10.1016/j.geothermics.2020.101910.

[11] Zhang, W., H. Min, X. Gu, Y. Xi, Y. Xing. 2015. Mesoscale model for thermal conductivity of concrete, Constr Build Mater. 98 (2015) 8–16. https://doi.org/10.1016/j.conbuildmat.2015.08.106.

[12] Khan, M.I. 2002. Factors affecting the thermal properties of concrete and applicability of its prediction models, Build Environ. 37 (2002) 607–614.

[13] ASTM, D 5334-14 Standard Test Method for Determination of Thermal Conductivity of Soil and Soft Rock by Thermal Needle Probe Procedure, 2011.

[14] S. ISO, 22007-2: 2015. Plastics–Determination of thermal conductivity and diffusivity–Part 2: Transient plane source (hot disk) method, International Organization for Standardization (ISO), Geneva, Switzerland. (2015).

[15] Carslaw, J.C.J. H. S.. 1959. Conduction of Heat in Solids, 1959.

[16] COMSOL Multiphysics®v. 5.3. 2015. COMSOL AB, Stockholm, Sweden.

[17] Kim, Y.S., H.B. Dinh, G.O. Kang, D.T. Hoang. 2023. Performance evaluation of a novel horizontal ground heat exchanger: Coil-column system, Journal of Building Engineering, 76 (2023) 107180. https://doi.org/10.1016/j.jobe.2023.107180

[18] ACI Committee 229R, Controlled Low Strength Materials (ACI 229R-99, American Concrete Institute, Farmington Gill, MI, USA, 1999.

[19] Kim, Y.S., H.B. Dinh, M.T. Do, G. O Kang. 2020. Development of thermally enhanced controlled low-strength material incorporating different types of steel-making slag for ground source heat pump system, Renew. Energy 150 (2020) 116-127, https://doi.org/10.1016/j.renene.2019.12.129.

[20] ASTM:C940-10a, Standard Test Method for Expansion and Bleeding of Freshly Mixed Grouts for Preplaced-Aggregate Concrete in the Laboratory, ASTM International. i (2010) 1–3.

[21] D. ASTM, 6103 (2004), Standard Test Method for Flow Consistency of Controlled Low-Strength Material (CLSM), American Society for Testing and Materials. (n.d.) 1–3.

[22] ASTM C39/C39M, Standard Test Method for Compressive Strength of Cylindrical Concrete Specimens 1, 2003. https://doi.org/10.1520/C0039_C0039M-21.

[23] Chang, K.-S., M.-J. Kim, Y.-J. Kim, A Study on the Determining Initial Ignoring Time for the Analysis of Ground Thermal Conductivity of SCW Type Ground Heat Exchanger, Korean Journal of Air-Conditioning and Refrigeration Engineering. 26 (2014) 453–459. https://doi.org/10.6110/kjacr.2014.26.10.453.

[24] S. ISO, 22007-2: 2015. Plastics–Determination of thermal conductivity and diffusivity–Part 2: Transient plane source (hot disk) method, International Organization for Standardization (ISO), Geneva, Switzerland. (2015).

[25] Ocùoñ, P., D. Taler, P. Cisek, M. Pilarczyk, Fem-Based Thermal Analysis of Underground Power Cables Located in Backfills Made of Different Materials, Strength of Materials. 47 (2015) 770–780. https://doi.org/10.1007/s11223-015-9713-4.

[26] Choorackal, E., P.P. Riviera, D. Dalmazzo, E. Santagata, L. Zichella, P. Marini, Performance-Related Characterization of Fluidized Thermal Backfills Containing Recycled Components, Waste Biomass Valorization. 11 (2020) 5393–5404. https://doi.org/10.1007/s12649-019-00650-9.

[27] Quan, L., C. Fu, W. Si, J. Yang, Q. Wang, Numerical study of heat transfer in underground power cable system, Energy Procedia. 158 (2019) 5317–5322. https://doi.org/10.1016/J.EGYPRO.2019.01.636.

[28] P. Ocłon, P. Cisek, M. Matysiak, Analysis of an application possibility of geopolymer materials as thermal backfill for underground power cable system, Clean Technol. Environ. Policy 23 (2021) 869–878, https://doi.org/10.1007/s10098-020-01942-8.